Comments on Inorganic Chemistry
Publication details, including instructions for authors and subscription information:
http://www.informaworld.com/smpp/title~content=t713455155

THE HELIX-TURN-HELIX AS A SCAFFOLD FOR CHIMERIC NUCLEASE DESIGN

Sonya J. Franklin[a]; Joel T. Welch[a]
[a] Department of Chemistry, University of Iowa, Iowa City, Iowa, USA

To cite this Article Franklin, Sonya J. and Welch, Joel T.(2005) 'THE HELIX-TURN-HELIX AS A SCAFFOLD FOR CHIMERIC NUCLEASE DESIGN', Comments on Inorganic Chemistry, 26: 3, 127 — 164
To link to this Article: DOI: 10.1080/02603590500201188
URL: http://dx.doi.org/10.1080/02603590500201188

Comments on Inorganic Chemistry, 26: 127–164, 2005

ISSN: 0260-3594 print
DOI: 10.1080/02603590500201188

Taylor & Francis
Taylor & Francis Group

THE HELIX-TURN-HELIX AS A SCAFFOLD FOR CHIMERIC NUCLEASE DESIGN

SONYA J. FRANKLIN
JOEL T. WELCH[†]

Department of Chemistry, University of Iowa, Iowa City, Iowa, USA

De novo **design is a powerful tool to investigate the active site of enzymatic metalloproteins, in a smaller, defined model system. It is also a way to build or combine activity and selectivity in unique ways, not seen biologically. We are utilizing protein design to build artificial endonucleases, and to investigate fundamental questions of metallonuclease structure and function. We have focused on designing peptide constructs comprising geometrically similar turns from unrelated proteins, in particular the Ca-binding EF-hand motif of calmodulin and the helix-turn-helix motif (HTH) of engrailed homeodomain. By substituting the calcium-binding (and thus lanthanide-binding) loop in place of the "turn" of engrailed HTH, hydrolytically active, DNA-binding constructs were created. The NMR solution structure of one La-binding chimera (P3W), calculated based on NOE volume integrals, demonstrated that the 33-mer peptide retains the parental helix-turn-helix structure when bound to lanthanide ions. The binding affinities of the chimeras for Ln(III) ions are in the low μM regime, typical for EF-hand sequences, despite the significant changes in flanking sequence. Importantly, the Ln(III) chimeras are catalytically competent, able to hydrolyze phosphate esters including DNA, and were found to bind and cleave DNA with sequence preference. Thus, these designed HTH/EF-hand chimeras represent the first examples of small peptidic artificial nuclease with sequence discrimination, and show**

[†]**Current address: Schering-Plough Research Institute, Kenilworth, NJ, USA.**

Address correspondence to Sonya J. Franklin, Department of Chemistry, University of Iowa, Room 373 CB, Iowa City, IA 52242, USA. E-mail: sonya-franklin@uiowa.edu

that the HTH is a robust scaffold on which to build novel metallopeptide constructs. This review describes the design and characterization of Ln-binding HTH/EF-hand chimeras.

A long-standing interest in the biochemistry of lanthanides, which often mimic calcium coordination, and a growing appreciation for the complexities of protein-DNA recognition led one author (SJF) to a surprising crossroad during the lecture of renowned Ca-protein expert Sture Forsén: the realization that the super-secondary "turn" structures of the ubiquitous Ca-binding EF-hand motif and the helix-turn-helix motif common to many DNA-binding regulatory proteins are essentially identical 90° helical turns. Why then doesn't calmodulin bind DNA? We set out to address this question, and to test the premise that the turn of these two motifs is modularly substitutable. Our goal is to develop tools to investigate fundamental principles of protein-DNA recognition, tuning of nuclease activity, and ultimately, to design selective nucleases for gene manipulation *in vivo* and on the benchtop. This review describes the design and characterization of lanthanide-binding, hydrolytically active peptides in our lab, based on EF-hand and helix-turn-helix motifs.

PROTEIN DESIGN AS A TOOL FOR BIOINORGANIC CHEMISTRY

Since proteins were first understood to be a fundamental molecular building block for life, the relationship of protein sequence and function has excited our imagination and curiosity. An implicit assumption of the study of protein function has been that these complex molecules assume well-defined structures, which allow them to perform and regulate crucial biological reactions.[1] Yet protein folding, dynamics, and tuning of enzyme activity involve many subtle, weak interactions, whose intricacies are only slowly coming into focus. The rich inorganic chemistry exploited by metalloproteins further expands the complexity of the reaction-space to be explored. As mimicry is the greatest compliment, an appreciation for the effortless and beautiful structures in nature leads to the desire to build and manipulate proteins for our own ends. In so doing, creating novel proteins that share both the function and the reactivities of the native Forms which they shadow represents a benchmark for our current level of understanding of protein behavior.

The incorporation of novel metal binding sites into proteins has long been a goal of *de novo* design, particularly focusing on the creation of minimalist active-site models for enzymes. Metal ions represent a versatile and tunable way for proteins to catalyze difficult yet biologically imperative reactions. Metal binding sites have been found in at least one–third of all structurally characterized proteins and are estimated to occur in half of all proteins as a whole.[2] The same metal cofactor can perform vastly different chemistry depending on context, and thus the creation of novel metal ion sites in proteins could potentially confer useful and unexplored new combinations of activities.

Much of the pioneering work in metalloprotein design has relied on robust scaffolds such as 3- and 4-helix bundles.[3–12] These alpha-helical bundle proteins have been the standard for understanding protein folding and for the rational incorporation of metal-cofactors promoting diverse chemistries. In addition, a number of computer–based algorithms (Dezymer;[13] Metal Search[14]) have been used to build organized metal-binding sites into a variety of protein scaffolds.[15–17] These studies have sought to explore what DeGrado has called the "molecular middle ground" between small synthetic analogs of active sites, a mainstay of bioinorganic chemistry, and native enzymes.[7] For example, Fe-heme proteins catalyze a range of fundamental biological reactions, including electron transfer and oxygen activation. Small-molecule porphryn complexes provide well-defined models of inner-sphere coordination for comparison with heme proteins, but much of the subtlety defining redox potentials, electron transfer, ligand exchange, and selectivity is imparted by the protein matrix. By rationally incorporating heme sites into known protein scaffolds, these synergistic, environmental influences on the metal active site are now being systematically defined. The redesign of heme proteins and construction of tunable heme sites in α-helical bundles have been among the most extensive and successful applications of metalloprotein design to date.[5,12,18–23]

Many other metalloprotein active sites besides iron-hemes have been explored with a number of elegant designed systems (for a recent review, see reference 18). Peptide and protein models of "blue copper" proteins (Type 1)[24,25] have been engineered to elucidate the role of the protein matrix in directing the coordination geometry of Type 1 or Type 2 Cu sites as well as their redox potentials.[26,27] Gray and Malmström postulated that not only the inner sphere coordination set, but also the structural constraints and H-bonding networks stabilizing these ligands

dictated blue-copper proteins' redox potentials.[28] Lu and Valentine's elegant demonstration of this principle by engineering the Cu-site of astacin into a blue-copper site tested and confirmed the generality of the effect.[26] More recently, Lu and coworkers have engineered a Cu-heme site into myoglobin, thereby mimicking the reactivity of heme-copper oxidase within a completely different framework.[29]

Tuning the same ligand set to prefer specific divalent ions or to use the same ion in divergent ways is a significant goal of protein design. For example, Sugiura and coworkers recently redesigned a structural zinc finger motif into a hydrolytically active site by varying ligand set (Cys, His, Asp) or by modifying the sequence to leave an open coordination site for water or substrate binding.[30] The modified zinc fingers hydrolytically cleaved amino acid esters[30] and DNA oligonucleotides.[31] The power of the protein matrix to deliver, orient, constrain, and electronically tune a set of donor groups is remarkable, and is now being exploited by chemists through protein design.

CHIMERIC DESIGN BASED ON MODULAR TURN SUBSTITUTIONS

We have taken a chimeric approach to protein design, which allows us to combine or create new functions by using known protein folds in novel contexts. As with the mythological Chimera of Greek mythology, the synergistic incorporation of seemingly unrelated parts generates a complex with function both derived from and unique relative to its parental components. This is reminiscent of genetic domain swapping, known to be a common occurrence in the evolution of proteins, but on the smaller scale comprising supersecondary motifs. We postulated that the similarity of certain ubiquitous turn structures could be exploited to modularly mix components with very different primary sequences, thus generating new motifs without altering the fold of the motif.

Within the context of utilizing design to unravel the subtleties of metalloprotein folding and tuning of function, we have used the goal of creating an artificial endonuclease as a design target. We have exploited the virtually identical supersecondary structure of two protein motifs (Figure 1), namely the EF-hand (a calcium binding motif), and the helix-turn-helix (a DNA-binding motif) to create chimeric metallopeptides. Both these structures comprise an α-α corner, a pair of orthogonal α-helices separated by a turn, which is a very common structural theme

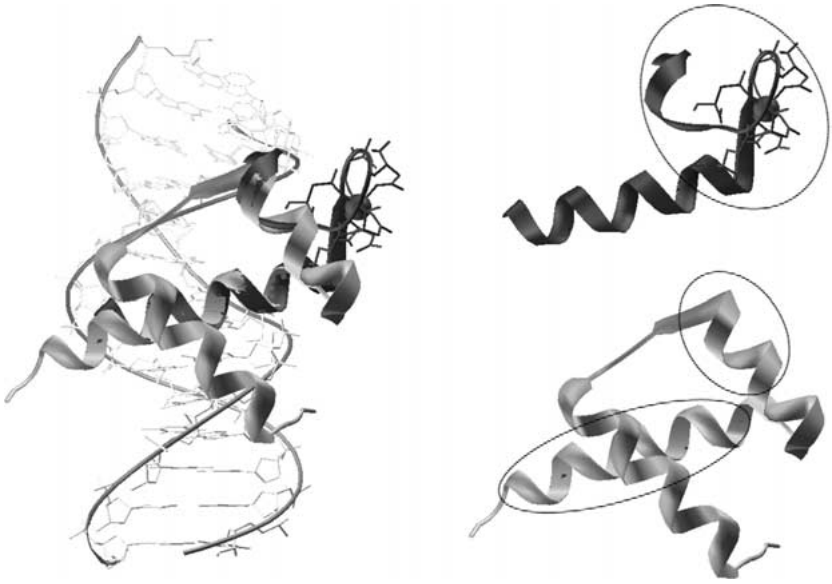

Figure 1. The structural similarities of a single EF-hand motif of *calmodulin* (1OSA; dark ribbon) and the HTH motif of *engrailed* homeodomain (1ENH; light ribbon) are highlighted in this overlay of known crystal structures (left). Our designed chimeric peptides comprise the Ca/Ln-binding turn (circled, top right) and the helices of the DNA-binding motif (circled, bottom right).

across the proteome.[32] We postulated that the "turn" sequence could be interchanged between α-α corner motifs, without compromising structure, metal-affinity, or DNA-binding ability of the parental domains. The ability to substitute entire structural elements (such as different metal binding loops and transcription factor sequences) offers the intriguing possibility of tailoring reactivity and targeting at will. Such combinations of functionalities could allow for tuning of catalyst substrate and efficiency, and even mechanisms depending on the intended function. With our first generation designs (Figure 2), we sought not only to determine if the premise of modular turn substitution was sound, but also to delineate the criteria for correct loop incorporation. These constructs have allowed us to begin to address the nuances of Ca-binding loop reactivity, affinity, and structure in a new context, as well as exploring the interactions of designed peptides with potential DNA recognition elements.

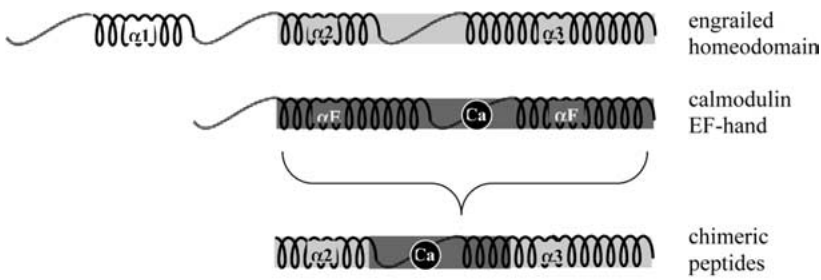


```
P2:       ERRRQQLSSEAETIFGDGDKDEIKIWFQNKRAK
P3:     TERRRQQLDKDGDGTIDERETIKIHFQNKRAKIK
P3W:    TERRRQQLDKDGDGTIDERETIKIWFQNKRAKIK
P4:     TERRRFRVFDKDGNGYISAAEKIWFQNKRAKIK
P4a:    TERRRFDKDGNGYISAAELRHVKIWFQNKRAKIK
P5b:    TRRRRFSLFDKDGDGTITTKEIWFQNRRAKWK
P5L:        FSLFDKDGDGTITTKEVWF
```

Figure 2. Top: A graphical description of our modular turn substitution design approach. The HTH motif of the homeodomain (α2 and α3; light gray) and the Ca-binding loop of an EF-hand (dark gray) were combined to give chimeric peptides. Bottom: The sequences of select chimeric peptides. Light gray (*engrailed* or *antennapedia*); black (*calmodulin* or EF-hand consensus). The 12-residue Ca-binding motif is underlined (reversed in control peptide P2).

In order to give context to our metalloprotein nucleases, in the following sections we will address the three main components of our chimeric design approach. Our chimeras synergistically incorporate Ca-binding, DNA-binding, and lanthanide-mediated nuclease activity.

BACKGROUND: EF-HAND MOTIFS AND THE DESIGN OF CA-SITES

The structural EF-hand motif is among the most commonly observed Ca-binding motifs in proteins.[33,34] The term "EF-hand" was first coined by Kretisinger and Nockolds as a pictorial representation of the orthogonal "thumb and forefinger" geometry of a pair of α helices, with a Ca atom grasped in the "palm."[35] This motif is exploited by signaling proteins to translate the information content of Ca(II) ion concentration into structural changes upon metal-binding, and calcium affinities therefore fall within the normal physiological range of calcium concentrations (10^{-5}–10^{-8} M).[34,36] In other cases, the motif apparently serves

primarily to stabilize a protein fold.[37] Notably, the Ca-EF-hand has only been observed in a structural, rather than catalytic role.

The classic EF-hand contains a twelve residue binding loop with Asp, Asn, Glu, and backbone carbonyl donor groups, with the consensus sequence $D_1X_2(D/N)_3X_4(D/N)_5X_6X_7X_8(D/N)_9X_{10}X_{11}E_{12}$.[33] The seven-coordinate site is roughly octahedral, if the bidentate E_{12} is considered as a single axis of the octahedron. The EF-hand ligand set is thus often designated with a Cartesian coordinate system to indicate the donor atoms' relative positions as the loop twists around the metal: X•Y•Z•(−X)•(−Y)••(−Z).[37] The −Z position is invariantly occupied by a bidentate glutamate, and the –Y ligand, sometimes referred to as the "gateway position,"[38,39] is involved in second-shell coordination and stabilization of a metal-bound solvent molecule. This ninth (–Y) position varies significantly among EF-hand loops, as it plays a fundamental role in regulating the kinetics of metal binding and release through a combination of sterics and hydrogen bonding. As a result, a 1000-fold difference is observed for the metal dissociation and association kinetics of various calcium binding sites.[33,34]

The EF-hand site is structurally versatile, allowing significant variation in affinity and function. The calcium binding affinities of EF-hands range over five orders of magnitude ($K_d = 10^{-4}$ to 10^{-9}), often recognizing calcium specifically over physiological metals with similar chemistry, such as Mg(II).[34] The amount of discrimination between ions varies greatly here as well, but the motifs typically favor Ca over Mg by approximately four orders of magnitude. For those sites in which binding serves merely a buffering (rather than signaling) role, discrimination is not required, and these proteins often bind Mg(II) under physiological conditions. However, EF-hands that serve specific regulatory functions must be able to bind Ca(II) tightly despite the large background concentration of Mg(II). Calcium binding usually occurs cooperatively in EF-hand proteins, since the EF-hand motifs occur in pairs and binding is coupled to significant structural rearrangement in most cases. The degree to which cooperativity is observed varies widely as well, and contributes to this discrimination.[37]

Because of the similarity of Ln(III) to Ca(II) in size, preference for hard oxygen donor ligands, and high coordination number (8 or 9 for Ln(III)), lanthanide ions bind tightly and isostructurally to calcium-binding loops of EF-hands.[40,41] This structural fidelity is well established, and means that the unique spectroscopic and magnetic

properties of the lanthanides are available to explore the chemistry of Ca-binding proteins.[42] The binding affinities fall in the low micromolar range, somewhat tighter than Ca(II) due to the increase in charge to size ratio, and the coordination sphere includes one or two additional water molecules. Thus there is a rich literature of Ln-chemistry that utilizes these rare earth ions to probe and characterize native EF-hand sites.

It is clear that delineating the aspects involved in tuning an EF-hand site for Ca, Mg, or Ln is a non-trivial task. Though hundreds of structures of EF-hand calcium binding proteins have been solved, the exact mechanism exploited by these proteins to achieve their affinity and selectivity for Ca(II) is still a matter of debate.[34,41,43,44] Calcium binding sites typically adopt either a pentagonal bipyramidal geometry or a distorted octahedral geometry. This structural variation produces sites that vary in coordination number and exhibit a wide range of bond lengths and angles.[45] Small peptides based on the sequences of native calcium binding sites in proteins have been studied for decades to unravel the systematic behavior of EF-hand sites.[46–48] These peptide studies have shown that Ca-binding helps to nucleate the C-terminal helix of the motif, and have served to delineate important residues involved in stabilizing the turn. Further, the native peptides spontaneously dimerize in solution, showing the strength of the back-to-back dimer interface that ubiquitously occurs between these motifs in proteins.[49]

The design of a Ca(II) site with strong affinity remains a difficult task and even, according to some, impossible.[41,50] However, Yang and coworkers have successfully incorporated a single Ca-binding EF-hand site into an immunoglobulin protein, which is not a native metalloprotein.[45] They have reproduced the structure and, importantly, the affinity of the site, but in the context of a single "hand." Additionally, Poulos and coworkers have reengineered a K^+-binding loop of ascorbate peroxidase within cytochrome c oxidase, generating a classic eight-coordinate calcium binding site with tight affinity and cation discrimination.[51] This work suggests some of the inherent subtlety involved in tuning the selectivity of these metal sites, as the replacement of a Thr by Asp (T192D) was necessary to confer Ca(II) affinity rather than K^+ affinity in the designed system.

In another notable example of calcium-site design, Imperiali and coworkers utilized the isostructural binding of Ca and lanthanides to develop a highly fluorescent peptide tag based on the EF-hand.[52,53] A combinatorial peptide library was selected for sequences that bound

Tb(III) tightly and excluded waters from the inner coordination sphere, thus preventing quenching of Tb fluorescence. The resulting selected sequence bound Tb(III) with $K_d = 57$ nM, and fluoresced strongly when irradiated with 280 nm light. The incorporation of a disulfide linkage from the residues immediately before and after the metal binding loop (-1, $+13$) further improved this affinity 30–fold. This dramatic improvement in the affinity of the site for lanthanides shows the potential of this type of structure to generate tight and selective active sites. Since there is no evolutionary pressure to create a Ca-binding site with affinity outside the physiological regime, there may yet be significant flexibility to optimize this sequence for tight binding.

BACKGROUND: HOMEODOMAINS AND THE DESIGN OF DNA-BINDING MOTIFS

Well-folded, small DNA-binding domains such as homeodomains and zinc fingers lend themselves well to protein design, and we and others have capitalized on such structures to investigate and manipulate one of the most fundamental partnerships in biology, the transcription factor protein domain associating with its target DNA recognition element. Creating novel DNA binding proteins has attracted a great deal of interest not only for its therapeutic potential, but also for its potential in molecular biology or proteome research. As a notable example, researchers at Sangamo, Inc., have successfully targeted and manipulated genes *in vivo* with designed zinc finger motifs, rationally chosen and strung together to bind tightly to a sequence of choice.[54,55] Schepartz has successfully designed a much smaller DNA-binding peptide, grafting the *engrailed* homeodomain recognition helix onto the avian pancreatic polypeptide (35 residues) with directed evolution techniques.[56] This tiny, well-folded peptide has affinity for its target site that rivals natural transcription factors ($K_d \sim 20$ nM). As mentioned above, in a particularly intriguing recent report Sugiura redesigned the zinc finger scaffold by removing an inner-sphere ligand, thus converting a structural site into a hydrolytically active one.[30] The Sugiura group has also achieved the remarkable transformation of one DNA-binding structure into another by redesigning a homeodomain to fold and function as a single zinc finger motif with only four amino acid substitutions.[57]

There is a limited set of structural motifs that nearly all DNA-binding proteins utilize to recognize and target DNA, including zinc-fingers,

leucine zippers, and helix-turn-helix (HTH) motifs. Of proteins containing these structures, homeodomains are of particular interest to us for a number of reasons. Not only is the helix-turn-helix motif a foundation for the outlined turn-substitution strategy, but this class of DNA-binding domains is also structurally and functionally well characterized, often binds DNA as a monomer, and the third helix has been implicated in membrane translocation as well as sequence recognition.[24,58–60] This suggests that a small, well-folded motif of this nature could have significant affinity for DNA and a built-in mechanism for cellular uptake. Thus a key aspect of our work is maintaining the integrity of the HTH fold as an element outside of a larger protein context.

Homeodomain proteins are a family of highly conserved DNA-binding proteins that regulate transcription and development in eukaryotes. The region that directly associates with and recognizes specific DNA sequences (the "homeodomain") comprises a highly basic, three helical bundle domain consisting of approximately 60 amino acids, with an N-terminal tail that wraps into the minor groove opposite the recognition helix. *Engrailed* homeodomain, the first homeodomain to be co-crystallized with DNA,[61] is a classic member of this family. This well-characterized protein from *Drosophila* targets the sequence 5′-TAATTA-3′. Like most DNA-binding proteins, homeodomains rely on the well-suited complementary surfaces of the α helix and the major groove of DNA.[62] The possibility of modulating the target sequence of a novel protein *via* subtle changes to the orientation or sequence of the recognition helix is of particularly interest for future designs and applications.

The essential DNA recognition element of the homeodomain is the helix-turn-helix, best described as a "motif" as this recurring substructure is not generally stable independent of a larger domain. Classically, the homeodomain's HTH comprises a helical segment of 10–11 residues, a five residue turn, and a 13 amino acid C-terminal helix, which lies in the major groove of DNA.[63] Key hydrophobic residues within α2 and α3 are crucial to the maintenance of the α-α corner structure, and usually interact with additional hydrophobic residues capping the motif (α1) to complete a compact hydrophobic core. Notably, the tryptophan in the third helix is rigorously conserved in all known homeodomains (with one exception),[24,64,65] and apparently plays a critical role in both domain structure and membrane translocation.[66,67] We have found in our work that this hydrophobic core, and the Trp in particular, are critical to the HTH scaffold when isolated from the full homeodomain as well.

BACKGROUND: LANTHANIDES AND DNA-HYDROLYSIS

The hydrolysis of DNA is a particularly difficult physiological problem given the stability of its phosphate ester bond, yet biological systems attain catalytic enhancements of up to 10^{15}-fold in hydrolysis rate (s^{-1}).[68] Typically this catalysis is achieved by activating both nucleophile (water) and substrate, often with the Lewis-acidic metal ions Zn(II), Ca(II) or Mg(II). In our efforts to understand and rationally tune enzymatic activity, we sought to duplicate this challenging feat with a much smaller, designed system. We chose the lanthanide ions both for their notable Lewis acidity and their isostructural binding to physiological Ca-sites such as EF-hands.

Lanthanides have been known to promote the Lewis acid mediated cleavage of phosphate ester bonds for decades, and in recent years they have been shown to catalyze the hydrolysis of DNA with remarkable efficiency compared to physiological metal ions such as Cu(II), Zn(II), Ca(II), and Mg(II). The lanthanides' higher oxidation state in aqueous solution (Ln(III)), inaccessible redox chemistry (>1.0 V to oxidize or reduce), rapid exchange kinetics, and spectroscopic handles make these ions well suited to activate artificial metalloenzymes.

A variety of approaches have been reported utilizing Ln(III) ions to develop artificial nucleases (recently reviewed, 69–71). Simple aqueous ions of lanthanides, despite being effective catalysts, suffer from low solubility in neutral-to-basic solutions, and their toxicity prevents direct *in vivo* applications. Therefore it is important to develop ligands that balance coordination and encapsulation with Lewis-acid activation and substrate accessibility. A diverse collection of small organic ligands has been exploited to explore this balance, including macrocycles, polyaminocarboxylate derivatives, crown ethers and even various mixed lanthanide-transition metal systems. Generally, polyaminocarboxylate ligands are less active, though more thermodynamically stable, so a great deal of interest lies in modulating Lewis acidity through substituting neutral hydroxyl ligands for carboxylates. Morrow and coworkers have had particular success with this approach utilizing a series of DOTA derivatives, which have been shown to hydrolyze oligonucleotides (RNA) with second order rate constants in the range $k_2 = 0.2$–$1.1\ M^{-1}s^{-1}$.[72–74] Both Morrow[75] and Komiyama[76] have demonstrated selective lanthanide-catalyzed hydrolysis with an antisense approach, by appending chelating ligands to oligonucleotides complementary to a target sequence.

Cleavage occurred specifically within 4–5 base pairs of the resultant duplex. Recently, Komiyama and coworkers have shown the power of Ln-hydrolysis by recruiting Ce(IV) ions selectively to a DNA single-strand gap bracketed by phosphate-derivatized duplex termini.[77]

Prior to our work, all Ln-mediated artificial nuclease were small molecule complexes rather than peptidic systems. We initially demonstrated that lanthanides were indeed hydrolytically competent in an EF-hand, the first example of catalytic activity by such a motif.[78] Our approach to selective DNA-hydrolysis is to target a double stranded DNA sequence using the same type of protein-DNA interface that transcription factors employ. This strategy allows us to use a physiological motif for lanthanide binding, thus delivering an active metal to a selective DNA-site.

THE DESIGN OF HTH/EF-HAND PEPTIDE CHIMERAS

Work in our lab has demonstrated that a nuclease can be designed based on the HTH scaffold, by generating small peptides comprising homeodomain and EF-hand sequences. We have utilized the concept of *modular turn substitution* to incorporate a metal-binding site into a DNA-binding motif, while retaining the structure and functions of each component (Figures 1 and 2). We have found these designed peptides have a well-defined solution structure, bind metals, bind and cut DNA with sequence preference, and enter cells in a metal-dependent way.

The HTH and EF-hand motifs consist of two helices at approximate right angles to one another, stabilized by conserved hydrophobic interactions along the helical inner surfaces. This "α-α corner" topology is a super-secondary structural motif common to many proteins.[4,32] A series of 33- and 34-mer peptides were designed based on overlaid crystal structures of the α-α corners of *calmodulin* (1OSA)[79] and the *engrailed* homeodomain (1ENH).[61] Known protein crystal structures were oriented manually using the program SwissPDBViewer,[80] to align the orthogonal helices of the homeodomain HTH motifs and various Ca-binding protein EF-hand motifs (*calmodulin, parvalbumin*). Generally, overlays show that 10 residues of the turn of the HTH must be replaced (for example S_{35}–Q_{44} of *engrailed*) to maintain collinear helices and key hydrophobic residues at the pivot of the fold. The best fits (by inspection and RMS deviations) were used to guide further peptide design. Recently, molecular mechanics models of loop insertions using the

protein modeling program Gromacs[81] have confirmed the relative loop orientation found with our peptide work to be optimal for minimal alpha-alpha corner perturbation (similar to P3W; unpublished data).

Several peptides with different relative orientations and sequences were constructed, the most successful of which in maintaining the parental α-α corner structure was peptide P3W. As shown in Figure 2, peptide P3W comprises helices $\alpha 2$ and $\alpha 3$ of *engrailed* (residues T_{27}–L_{34} and I_{45}–K_{57} respectively), with the turn region replaced by the consensus Ca-binding EF-hand loop. A very similar peptide (P3) was constructed with a single Trp_{24} to His_{24} substitution. This small change resulted in a significantly impaired fold, highlighting the importance of maintaining the hydrophobic core of the HTH motif. Additionally, important hydrophobic interactions known to stabilize EF-hand structures[37] were retained before and after the 12-membered binding-loop (at the -1, $+13$, and $+16$ positions), though the residues derive from the *engrailed* sequence (L_8, I_{21}, and W_{24}). The importance of the deliberate coincidence of the key hydrophobic contacts between the two turn motifs is a fundamental (if obvious) result of our modular turn substitution studies, and parallels similar conclusions with α-helix bundle heptads.[7]

In addition to P3W, several other peptides were investigated, varying both the sequences of the Ca/Ln loop and the helical regions (for example, P5b is derived from *antennapedia* rather than *engrailed* homeodomain; Figure 2). These peptides retain metal-binding function, reactivity and some helicity, but are less structurally organized than P3 or P3W (*vide infra*). We now conclude this is due to a less than ideal loop orientation, which compromises the hydrophobic "core" of the fold. Additionally, peptide P2 was designed as a control for binding and folding. P2 comprises sequence regions similar to P3W, but with the EF-hand loop register backwards, which allows us to distinguish weak electrostatic binding to the many Asp ligands from binding to an organized EF-hand consensus with concomitant nucleation of helicity to either side of the loop.

METAL ION AFFINITY AND BINDING PREFERENCES

In order to determine whether turn-mutated HTH peptides retained the ability of EF-hands to bind Ca and Ln, the binding affinities of the chimeric peptides with various trivalent Ln(III) ions and Ca(II) were determined. Although the range of affinities was much smaller than for

calcium proteins, the low micromolar affinities are similar to that of many native EF-hand sequences. The periphery or context of the loop thus did not fundamentally alter the affinity for Ca and Ln, despite changes in sequence and, importantly, overall charge of the flanking helices.

Peptide affinities were determined to be in the low micromolar range by following changes in the intrinsic fluorescence intensity of tryptophan as a function of added metal.[78,82,83] All the peptides (save P3) contain at least one tryptophan residue within the DNA recognition helix (the C-terminal helix of the HTH motif). Even in the context of these small "half-domain" peptides, this hydrophobic residue undergoes a considerable change in local environment upon folding, and is thus a sensitive reporter of metal binding. The titration data were iteratively fit to a 1:1 association model to determine K_d.[83,84]

The fluorescence of tryptophan is exquisitely sensitive to solvent exposure and hydrogen bonding effects. Typically, Trp emission is enhanced upon folding and accompanied by a blue shift, due to the fluorophore moving from a solvent exposed, hydrophilic environment into a more protected, hydrophobic core. However, Trp in the native *engrailed* domain is instead dramatically quenched upon folding.[85] This has been proposed to result from organized electrostatic interactions between Trp and a structurally conserved water molecule roughly normal to the indole plane, that pack and stabilize the interior corner of the HTH. This interaction in turn is proposed to lead to a more facile excited state electron transfer to peptide bonds, and subsequent fluorescence quenching.[86,87] With our chimeric peptides we similarly observe a quenching rather than enhancement in Trp emission upon metal binding (though smaller in magnitude than for *engrailed*). This suggests (and is supported by CD data) that metal-binding drives peptide folding and the adoption of a local Trp environment similar to the native α-α corner motif. The local structure of the turn is thus reasonably robust.

In addition to fluorescent titrations, several alternate methods were employed to determine or verify the binding affinities. Eu-luminescence titration experiments (*vide infra*), isothermal titration calorimetry experiments, and for those peptides that folded extensively, ^{1}H NMR and circular dichroism titrations are in good agreement with the values determined by Trp fluorescence titrations. It should be noted that in most cases these values are conditional dissociation constants, determined in the presence of the weakly chelating buffer Tris

(tris(hydroxymethyl)aminomethane; $K_{d(LnTris)} = 4$ mM).[88] This allowed titrations and activity assays (*vide infra*) to be undertaken at neutral and slightly basic pH without lanthanide precipitation, but also slightly raises the dissociation constant we measure.

Binding affinities of the chimeric peptides for lanthanides were found to range from $K_{d(Eu)} = 1 \pm 0.3\ \mu M$ (EuP3W/EuP3) to $15 \pm 2\ \mu M$ (EuP4), with Ca(II) affinities approximately an order of magnitude weaker ($K_{d(CaP3W)} = 36 \pm 2\ \mu M$). This is presumably due to the calcium ion's smaller charge to size ratio, and is typical of Ca/Ln-binding EF-hand peptides generally.[47–49,89,90] In addition, we find no evidence of Zn(II) or Mg(II) binding, estimating affinities as in the mM regime.[91] These affinities for lanthanides place our peptides among the stronger small peptide Ln-complexes. This is perhaps somewhat surprising considering that not all of the peptides are extensively helical flanking the binding site. However, this may be an inherent feature of the higher valent lanthanides binding to the structurally malleable EF-hand site, both effectively balancing ligand charges and allowing facile reorganization around the metal center without significant loss of baseline affinity.[34] Note that unlike a free peptide, in the context of a full EF-hand protein (such as *calmodulin*), the free energy of long-range protein folding contributes to cooperative changes in Ca affinity and to maintaining the rigid "cage" of ligand around the metal site. The remarkable discrimination among ions *in vivo* (Ca(II) vs. Mg(II), Zn(II), K(I), Na(I)) has been suggested to stem both from ion size- and charge-selectivity in compensating negatively charged donor atoms.[34,92] The same may prove to be true for these chimeric HTH/EF-hand systems in the context of a larger protein as well.

STRUCTURE OF THE DESIGNED MOTIF

A critical test of our turn substitution postulate was the design of a motif that retained the α-α corner super-secondary structure. The observed quenching of Trp fluorescence upon metal addition suggested that at least local structural changes were occurring as the chimeras bound Ln(III) ions. We sought to determine whether the designed peptides would fold, and if so, to what extent the chimeras mirrored the parental domains.

We investigated the series of designed peptides by circular dichroism spectroscopy (CD) to determine global structural changes upon metal

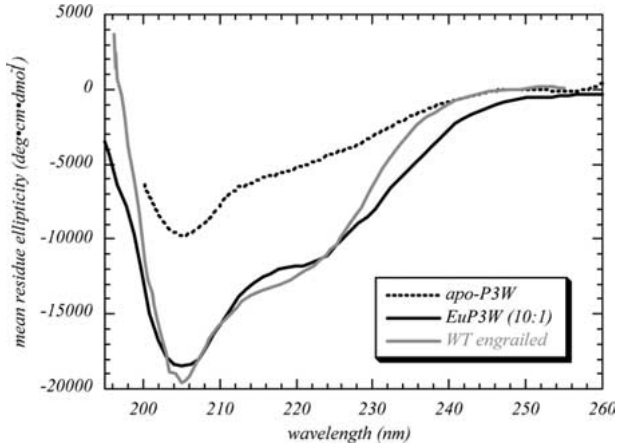

Figure 3. Circular dichroism spectra comparing similarities in secondary structure content of the folded metallopeptide EuP3W and WT-engrailed (engrailed data extracted from Figure 1, Mayor et al., Ref 94).

binding. As illustrated in Figure 3, P3W folds into a substantially alpha helical species upon coordinating lanthanides (Eu(III) shown). The extent of the helicity approaches 40%, calculated based on estimates of mean residue ellipticity at 222 nm,[93] and the CD spectral features mimic those of the *engrailed* parent.[94] In contrast, designs that either lack key hydrophobic residues within the putative helical regions of the peptide (such as P3, which lacks the key Trp_{24} residue,) or which possess these residues slightly out of register, (such as P5b with a Trp at +14 rather than +13 or +16, and P4a, which could muster only one turn of an α helix to the N-terminal side of the metal binding loop) display a much smaller propensity to be helical on average, as reported by the CD spectra. However, with the addition of trifluoroethanol (TFE), a solvent which tends to increase the relative amount of secondary structure by favoring internal hydrogen bonds over those with the solvent,[95] CD spectra can be obtained that approach the helicity for the well-folded P3W or *engrailed* itself.[82,83] This substantial increase serves to demonstrate that peptides P4a and P5b can access the predicted, folded secondary structure, but are not inherently as structurally stable or organized as P3W. Notably, control peptide P2 has little secondary structure, and the addition of up to 10 equivalents of Eu(III) does little to alter the relative amount of helicity. With the order of the metal-binding sequence

inverted, the required ligand residues are present but no longer organized to a consensus EF-hand structure.

The structure of the most helical of the metallopeptides (Ln(III) P3W) was investigated in more detail by ^{1}H-NMR. Paramagnetic broadening and shifts of most protons from residues 9–20 served to define the metal-binding loop of the Eu(III)P3W and Yb(III)P3W complexes. An increased signal dispersion relative to apo-peptide upon addition of diamagnetic La(III) indicated a transition from random coil to more secondary structure. Particularly notable were the shifts of hydrophobic residues before and after the loop (-1, $+13$, $+16$), in agreement with shift magnitudes and directions reported for other EF-hand peptide complexes upon Ca-binding.[96–98] More generally, the chemical shifts of alpha protons along the backbone are diagnostic of secondary structure context.[99] By calculating αH shifts relative to tabulated random coil values,[100] a histogram of average secondary structure was constructed. This chemical shift index method showed that LaP3W comprises a helix-loop-helix, with a short beta-strand run within the loop, as designed.[78]

A solution structure model of LaP3W was constructed from NOE constraint data, and confirmed that the designed system was a true helix-loop-helix (Figure 4).[78] The metallopeptide is well-defined from residues 8–25, with RMSD of only 1.05 Å for the 11 best structures (backbone atoms). 2D-NOESY, COSY, and TOCSY data were collected and peak assignments were made for most residues. The degeneracy in Lys and Arg residues (10 of the 33 total residues) resulted in a number of residues that could be assigned to spin systems but not definitively within the sequence (Arg_3, Arg_4, and Arg_5, for example). This along with the inherent flexibility of the parental WT-engrailed homeodomain[94] (and peptide termini generally) resulted in a model that was poorly defined at either end. Unlike many helical structures such as leucine-zipper-derived peptides or *de novo* alpha-helical bundles previously reported, the chimeric HTH metallopeptides are designed to have orthogonal, rather than parallel (or anti-parallel) helices, which would be stabilized along their entire length.[4] This difference likely exacerbates the disorder at the peptide termini.

Notable close contacts between Leu_8 and Ile_{21} and Trp_{24} were critical to defining the overall fold of the NOE-based model. Besides providing substantial thermodynamic driving force for the folding of this metallopeptide, these residues also serve to preserve the relative distances and orientations of the two helices, and thus the integrity of

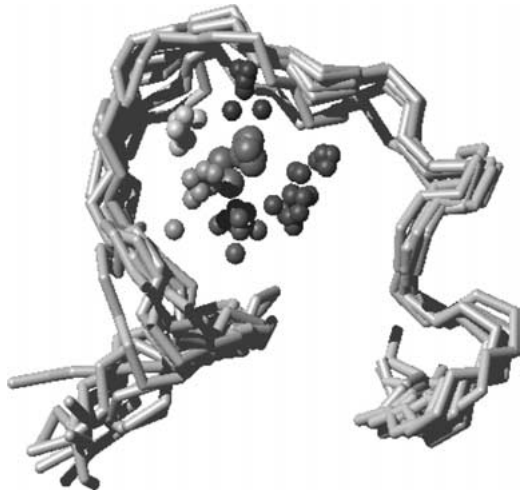

Figure 4. NMR solution structure of LaP3W, showing that it adopts the basic helix-loop-helix structure as designed (though termini are disordered).[78] The 9 lowest energy conformers (DYANA f-values) for the central region of the metallopeptide are shown (residues 7–26). La(III) is shown in larger spheres, and the ligating oxygens of Asp9, Asp11, Asp13, Thr15 (backbone), and Glu20 (bidentate) are shown in smaller spheres.

the overall fold. In parallel to previous reports with EF-hand peptides (*vide supra*), this cluster of key hydrophobic residues anchor the pivot of the α-α corner motif. Furthermore, in homeodomains, the Trp residue is nearly invariant, and is involved in both structure and function (membrane translocation, recognition).[24,25,65] As discussed above, P3, which has a Trp→His substitution within this anchoring triad, has less overall helicity, apparently due to more conformational flexibility at the turn. This conclusion is based on the smaller ^{1}H-NMR signal dispersion exhibited by LaP3 relative to LaP3W, and the two conformations experienced by His_{24} and adjacent Phe_{25}. These residues of LaP3 exhibit two chemical shift environments for both backbone and sidechain protons, which are in slow exchange on the NMR timescale. In contrast, all residues of LaP3W are well dispersed and exhibit only one chemical environment.

One particularly intriguing result of this structural study is that, unlike native EF-hands, LaP3W does not appreciably involve the ninth residue of the loop (Asp_{17}) in stabilizing a coordinated water molecule, leaving the metal-binding site very exposed in solution. We modeled the metal-binding loop both with and without explicit bonds (defined

lengths but not angles) to the putative oxygens of the coordination set and found the overall fold was unchanged. However, the fit was improved with explicit bonds to all but Asp_{17}, which could be reasonably modeled either toward or away from the metal center. The fit was marginally better modeled with Asp_{17} directed away from the metal, perhaps because of the additional degrees of freedom along this extended loop in our monomeric EF-hand-like chimeras relative to native EF-hands, which occur ubiquitously in back-to-back pairs.

COORDINATION ENVIRONMENT OF LANTHANIDES IN THE HTH/EF-HAND CHIMERA

The solution structure of the designed metallopeptide LaP3W demonstrated the feasibility of modular substitution of these structural elements and the ability of the α-α corner to retain a predictable overall geometry. However, if these metallopeptides are predisposed to bind to the major groove like the parental HTH structure, the folding thermodynamics and coordination set of the metal ion may be affected by its interaction with nucleic acids. Although we determined the metallopeptide was well ordered in the absence of DNA, the signal resolution available with unlabeled materials and solubility issues prevented direct NMR studies to address these questions. Thus we could not determine whether metal-coordination was compromised upon binding to DNA by NMR. We sought to address this issue through the use of Europium (III) $^7F_0 \rightarrow {}^5D_0$ excitation spectroscopy.[101] This powerful technique allows the direct interrogation of the Eu(III) ion in the context of large protein or nucleic acid biomolecules, and has been used extensively to characterize EF-hand proteins as well as small molecule chelates.[42,102–104]

Eu-luminescence spectra report on the number of europium coordination environments (each singlet is a unique Eu environment), the coordination set (based on energy of the transition), and the number of coordinating water molecules (lifetimes of the transitions in H_2O vs. D_2O). At least two peaks are observed for each chimeric peptide (~579.3 and 579.7 nm). These transitions occur together in slightly different ratios for each metallopeptide. In all cases, the transition energies of these peaks are typical for a traditional EF-hand ligand set (six oxygen donor atoms from the EF-hand loop, plus water molecules), based on the correlation between transition energy and nephelauxetic parameters for the ligating atoms.[104] Eu-titrations showed the peaks growing in

together as a function of metal, and the data (sum) fit well to a 1:1 association model. Binding affinities determined by this method corroborated the values determined by Trp fluorescence titrations *(vide supra)*.

Although we know from titration and structural studies that only one Eu-binding site is available, the Eu apparently populates two very similar, exchanging ligand environments. This is consistent with the pairs of Eu-luminescent peaks that have been observed in both native EF-hand proteins and a variety of small molecule Eu-species,[105–108] which have been assigned to pairs of isomeric metal environments with equivalent sets of ligands organized with slightly different symmetry about the metal. This is also consistent with our NMR data indicating the structurally flexibility of the loop and "gateway" residue Asp_{17}. Alternately, these two peaks may represent two different hydration states (579.3 nm with 2 waters; 579.7 nm with 3 waters), although the lifetimes of the overlapping bands could not be differentiated to confirm this postulate.

The number of inner sphere water molecules was determined from emission lifetimes in D_2O and H_2O.[101,104] The hydration number (q) was found to be approximately $q = 2$ for most of our chimeric peptides, resulting in an eight-coordinate metal site. The exception was EuP5b, which has a slightly higher value ($q = 2.6 \pm 0.2$), implying that the Eu ion is more exposed than in the other systems. This is consistent with the flexibility and poorer folding observed by CD for EuP5b.

Upon the addition of DNA, the metal binding site is maintained, as the q value is approximately constant for the well-folded EuP3W species, and decreases to $q = 2$ for the more flexible P5b. This important observation is consistent with DNA serving to organize rather than compromise the integrity of the fold. If the peptide drastically unfolded or changed structure upon DNA binding such that the Eu-binding site was significantly altered, the ligand set and hydration number would approach that of aqueous Eu(III). It is also notable that no new DNA-dependent transitions occur upon the addition of the nucleic acid. This indicates that there is no significant change in the Eu coordination sphere, such as direct bonds to phosphate oxygen of the DNA backbone, although the relative ratio of the peaks changes slightly to favor the 579.3 nm peak. Presumably the equilibrium between structural isomers or toward a hydration number of 2 is altered by DNA (groove) binding.

In some metallopeptide spectra, a third peak of significant intensity was observed at higher energy (578.9 nm). This peak was pH-dependent and absent in all Eu-peptide spectra at pH 5. The third peak was

observed at pH = 7 for P4a and P5b, but and not until pH = 8 for P3 and P3W. Such a pH-dependent peak had previously been reported for Eu-loaded native EF-hands, and had been assigned to the deprotonation of a first coordination sphere threonine or serine.[109] However, we observed this behavior with P3 and P3W, which lack such a deprotonatable group in the first coordination sphere, and thus we assigned the pKa to the deprotonation of an inner sphere water. This pKa varied modestly (from pKa = ≈7.0–7.5) depending on the peptide's ligand set. Remarkably, the only difference between the coordination environment of EuP3W and EuP5b is the second shell "gateway" ligand (residue +9), yet in analogy to enzymes such as carbonic anhydrase,[110] the ligands adjacent to the metal center modulate the reactivity of the activated nucleophile (water). Moreover, the pKa is modulated upward by the binding of the metallopeptides EuP3W and EuP5b to DNA, which is expected in the presence of a polyanion. The observed pKa trend for this deprotonation process correspond reasonably well to the reported nuclease activity for our peptides (*vide infra*).

PHOSPHATASE AND NUCLEASE ACTIVITY

Although the Ca EF-hand is strictly a structural motif, we postulated that a monomeric Ln-binding EF-hand analog was catalytically competent. To test this hypothesis, we characterized the ability of the Ln-peptides to cut both nucleic acids and the activated DNA analog, bisnitro-phenylphosphate (BNPP). BNPP, an activated phosphate ester, is an attractive model bis-phosphate given the strong 400 nm absorbance of the nitrophenylate product and greater reactivity than DNA. The bright yellow product allows the reaction to be followed spectrophotometrically. Initial rates of BNPP cleavage were measured over a range of peptide concentrations, with excess substrate and less than 10% conversion. Under the tested conditions (20 μM metallopeptide in Tris buffer, pH 7.7), the rate of cleavage of $EuCl_3$ was ~20-fold less than that of EuP4a.[111] This important observation showed that the metallopeptide and not simply the aqueous or Tris-complexed ion was responsible for reactivity.

We find that the chimeric HTH metallopeptides can hydrolytically cleave both BNPP and nucleic acids, with rates that depend both on metal ion and on peptide sequence. Among the trivalent lanthanides, Eu(III) was generally the most active, though the trend in rates did not track consistently across the series: Eu > La > Tb ≈ Yb ≈ Lu >

Pr > Dy > Gd (for 10–40 μM Ln(III)P4a, 2.5 mM BNPP, pH 7.2, 10 mM Tris; Sirish and Franklin, unpublished results). A comparison of various peptides with the same metal ion (Eu(III)) showed the cleavage tracked with ligand set and DNA-affinity rather than structure. Peptide EuP4a is more active than EuP5b, EuP3W, or EuP3. The main factor directing this activity seems to be ligand set. As addressed above, Eu-luminescence experiments showed that the relative charge of the primary and secondary ligands serve to modulate the pK_a of a coordinated water molecule, which is the presumed nucleophile. The cleavage experiments were performed near neutral pH, where differences in these pKa's are most obvious. At pH 7.5, EuP3W is partially deprotonated (pKa ≈ 7.5), whereas the water of EuP4a is nearly fully deprotonated (pKa < 7).

To test whether a deprotonated nucleophile is involved mechanistically in hydrolysis, we determined the pH-dependence of BNPP cleavage by EuP5L. P5L is a small, 20 amino acid peptide comprising the central region of P5b (the calcium binding loop with one turn of the C-terminal helix), which allowed us to address the catalytic potential of the Ln-binding loop alone. A pH profile of BNPP hydrolysis showed this species had a modest increase in cleavage rate at pH 8.2 (note that BNPP has pKa of 6.9,[72] so this rate-enhancement is apparently peptide-dependent rather than substrate–dependent). Presumably this rate increase reflects the deprotonation of a coordinated water molecule responsible for the nucleophilic attack of the phosphate ester bond, since it agrees reasonably well with the pKa values determined for these chimeric systems from luminescence studies (*vide supra*).

We speculate there may be other factors influencing the order of activity of various Eu(III)-peptides, including aggregation and substrate recruiting. EuP3 was found (by NMR) to have a modest propensity toward dimerization at concentration greater than 200 μM while other metallopeptide chimeras do not.[82] Most likely, this dimerization results in a decrease in the solvent exposure of the metal center and a subsequent decrease in the relative amount of catalysis. Additionally, the presence of a hydrophobic residue (Tyr_{13}) in the case of P4a in the metal binding loop might serve to help draw the aromatic BNPP substrate more efficiently to the metal center. Residue substitutions to systematically test these postulates are ongoing.

The catalysis of BNPP illustrates that the monomeric Ln-bound HTH/EF-hand peptides are hydrolytically active phosphatases, the first

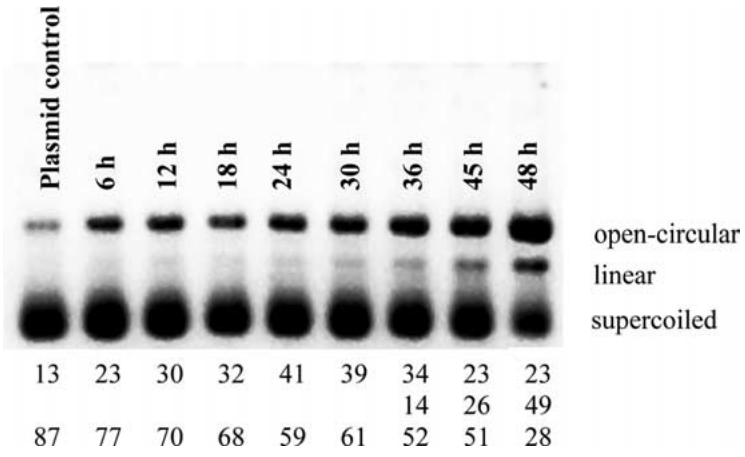

Figure 5. Agarose electrophoresis gel showing the cleavage of supercoiled DNA by EuP4a, 1:1; 12.5 μM (as in Sirish, et al., reference 83). The reactions were carried out in 50 mM Tris, pH 7.0 and the samples were incubated at 37°C for the given time periods prior to electrophoresis (0.5 × TBE, pH 8.0). Quantified intensities of open circular, linear, and supercoiled bands are given below (as % of total DNA). One anomalous time point (42 hrs) was omitted for clarity.

examples of an active EF-hand site. However, DNA is a more stable, and thus more challenging substrate than BNPP. To test the activity of the Ln-chimeras toward nucleotides, agarose gel electrophoresis experiments were used to determine the ability of the peptides to cleave supercoiled plasmid DNA (Figure 5.; Sirish and Franklin). These experiments demonstrated that our metallopeptides catalyze cleavage of supercoiled DNA to open-circular DNA, which suggests single strand cuts (some linearized DNA was also observed in the most active cases, which is presumably due to multiple single strand cuts). As with the BNPP model compound, the activity of the metallopeptide was greater than that of $EuCl_3$ (Eu-Tris) under the same conditions, and varied according to peptide sequence.

Ln-mediated DNA hydrolysis often involves Lewis-acid activation and deprotonation of an inner-sphere water nucleophile, and/or activation of the substrate P=O bond through phosphate coordination to the metal.[70] The NMR structure of LaP3W shows that the metallopeptide has several open coordination sites for substrate binding and for labile water exchange, but Eu-luminescence studies gave no evidence

of direct phosphate-Eu bonds. An isolated EF-hand-like structure thus apparently has enough accessibility of the active site metal to promote nuclease ability, even without bound substrate.[111]

DNA BINDING, TARGETING, AND CLEAVAGE

The intriguing nuclease activity of the Ln-chimeras that we observed raises the question of selectivity. Does a small metallopeptide comprising roughly half a DNA-binding domain have sufficient tertiary (or supersecondary) structure to interact with DNA as an organized unit, and thus have a preferred orientation leading to selective binding and cleavage? We initially determined that the chimeras have reasonable non-specific binding affinity for DNA (10–20 μM), through both agarose gel shift assays of plasmid DNA,[82,112] and CD studies of binding to a self-complementary 14-mer duplex.[91] We then examined the sequence preference of DNA cleavage by LnP3 and LnP3W with linearized ^{32}P-radiolabeled nucleotide duplexes.[112]

Fragments of plasmid DNA (120–250 b.p. in length) were excised with restriction enzymes, either 5′- or 3′-radiolabeled, and gel purified prior to incubation with the metallopeptides. Maxam-Gilbert sequencing lanes were included in the PAGE analysis to calibrate the sequence. We chose to use the very strong Lewis acid Ce(IV) (added as a freshly prepared aqueous solution of the $(NH_4)_2Ce(NO_3)_6$ salt) rather than the trivalent lanthanides, due to its greater reactivity.[113] Although the Ce(IV) is small compared to the trivalent lanthanides, we found by circular dichroism and Trp-fluorescence studies that the chimeric peptides bound this ion as well, with concomitant increase in helical structure.[112]

To test whether we were observing oxidative or hydrolytic cleavage, Maxam-Gilbert (3′-phosphate termini), DNase I (3′-hydroxyl termini), and FeEDTA/H_2O_2 (3′-phosphate and phosphoglycolate termini) control lanes were included to determine the fragmentation pattern of both aqueous Ce(IV) and the Ce(IV)peptides.[112] We found, in agreement with both Que and Komiyama's earlier reports[71,114,115] that aqueous Ce(IV) hydrolyzes rather than oxidizes DNA, leaving both 3′-hydroxyl and 3′-phosphate termini (comigrating with the DNase I and Maxam-Gilbert lanes, respectively; the complementary termini were observed with 3′-labeled nucleotide). Although Ce(IV) is slowly converted to Ce(III) in aqueous solution,[115] it is apparently a strong enough Lewis acid to hydrolytically rather than oxidatively cleave nucleotides.

In contrast to the double bands generated by the aqueous ions, Ce(IV)P3 and Ce(IV)P3W exhibit an apparent regio-preference in their cleavage mechanism. With the metallopeptides, only 3′-phosphate termini are observed with 5′-labeled DNA. This clearly indicates a different mechanism is in play than with uncomplexed metal ions. However, it was rather surprising that cleavage of 3′-labeled fragments also left only 5′-OPO_3 termini instead of the expected 5′-OH complement. This implies the loss of the intervening sugar (through either multi-step hydrolysis or *via* oxidative cleavage) rather than the simple addition of water across the phosphate-sugar bond. Although we did not observe phosphoglycolate termini, we cannot rule out the possibility that in the presence of the peptide, Ce(IV) promotes oxidative cleavage instead. However, hydrolytic cleavage patterns with Eu(III)P3W, which cannot readily access oxidative chemistry, were much weaker but appeared to give phosphate termini consistent with the Ce(IV)P3W results.

In addition to the difference in mechanism, the other notable observation from these experiments is a distinct sequence preference in cleavage by the metallopeptides. At low concentrations of Ce(IV)P3W (and to a lesser extent, the less organized Ce(IV)P3), some sequences are preferentially cleaved, and this effect is "washed out" at higher metallopeptide concentrations. On the particular fragment discussed in Kovacic et al.[112] cleavage was observed at the 5′-thymidine of the 5′-TCACC-3′ sequence. This cleavage pattern at lower concentrations suggests sequence recognition in binding (and thus cleavage), since the higher affinity sites are occupied first. Then as the concentration increases, all site are bound randomly and a ladder-pattern results. Such a cleavage pattern indicates that the metallopeptide must bind to DNA as a structured, folded unit, which presents an organized interface that results in discrimination among sequences. Although we found no evidence for recognition of 5′-TAATTA-3′, the consensus sequence targeted by the parental *engrailed* homeodomain, significant differences in target sequences are not unexpected. Even with a well-folded metallopeptide, the orientation of the recognition helix within the major groove is likely to be altered in the absence of the anchoring N-terminal tail and α1 (see Figure 1).

In order to determine the consensus binding site or family of sites of our chimeric peptides, we employed an iterative approach, coupling a gel-shift assay with PCR amplification of a library of sites (manuscript in preparation). A synthetic DNA oligonucleotide and complement were designed with PCR primer sequences at either end, and a library of

randomized octamer sequences in the center. For each chimera, a peptide concentration gradient gel-shift assay was performed in the presence of Ca(II), the ^{32}P-radiolabeled DNA visualized, and the shifted band (corresponding to approximately 50% bound) was excised. The extracted and purified DNA was again amplified with labeled primers, and the process repeated. After several rounds, the fragment was subcloned into a standard plasmid and sequenced. For CaP5b, a family of sequences was identified (5′-$^{A\text{-}C}_{/G}$-C-$^{T}_{/C}$-A-$^{T}_{/C}$-3′) and CaP3W was found to target and bind two sequence families, one of which is very similar to the cleavage target observed for CeP3W (binding: 5′-ACCCT-3′; cleavage: 5′-TACCTA-3′). This allowed us to corroborate the postulate that the cleavage preference was dependent on a binding site preference, and not simply on greater accessibility of some sequences to random cleavage. Interestingly, under acidic conditions, which partially serve to depurinate the DNA, both EuP3W and CeP3W begin to target and preferentially cleave these abasic A and G steps, but not the adjacent T bases recognized by the folded metallopeptide.[112]

Although not truly *specific* as a complete domain would be, this sequence *preference* in cleavage is remarkable and unprecedented for an underivatized peptide of this size. There are very few examples of small (<40 residue) peptides that even fold and bind selectively to DNA, let alone exhibit activity (Schepartz's modified avian pancreatic peptide protein[116] and Frankel's optimized single zinc finger[117] are notable examples). Conversely, examples of artificial nucleases are typically not based on folded, small peptides, or have additional functionality to promote binding or selectivity. For example, selective, lanthanide-mediated hydrolysis has been reported previously by Komiyama, either utilizing a 15-mer DNA oligonucleotide with a 5′-iminodiacetate-chelated Ce(IV) ion,[76] or adding complementary, terminally derivatized DNA "primers" to generate a single strand gap to recruit free Ce(IV) ion to the exposed region.[77] Additionally, Barton and coworkers have reported targeted DNA cleavage with a Zn(II)-binding peptide appended to a Rh-intercalator complex, which serves to deliver the peptide to the DNA.[118] Recently Sugiura has also achieved specific cleavage with a larger designed system, comprising three modified zinc-finger motifs (95 residues).[31,119] This is a beautiful example of redesign of a metal site to generate new reactivity, while retaining DNA affinity and selectivity. Like Sugiura's proteins, our much smaller chimeric metallopeptides interact with DNA as a defined, folded unit, both binding to

and cleaving DNA with sequence discrimination. Thus they represent the first catalytic EF-hand as well as the initial example of a metallopeptide "endonuclease."

OTHER APPLICATIONS OF HTH/EF-HAND CHIMERAS: MR CONTRAST

In the last two decades, Magnetic Resonance Imaging (MRI) has revolutionized clinical diagnosis, in large part because of the battery of Gd(III)-contrast agents now available to physicians that add sensitivity to this non-invasive technique. Now, as magnet technology becomes better and the pixel resolution approaches cellular dimensions, intriguing new applications for MRI are unfolding. Switchable, targeted agents are of interest to correlate enhanced contrast to biological events. Louie et al. have shown that it is possible to study an enzymatic signature during differentiation and development using MRI.[120] The ability to follow transcription of a specific gene in living systems and in real time would be a powerful complementary tool for developmental biology. Therefore an agent that could selectively bind DNA or RNA during expression may allow cells or collections of cells to be imaged as they are involved in gene transcription.

As an initial test of a pilot system and a basis for further design, we tested whether Ln-binding HTH/EF-hand chimeras might serve as MRI contrast agents.[121] Unlike most bifunctional contrast agents being developed that append the targeting vector or binding motif to the metal-binding site through a linker, this system incorporates the Gd site within the DNA-binding and targeting unit. This unique structural approach limits the rotational flexibility and internal motion of the Gd center and may thus increase relaxivity. Moreover, increased rigidity and slower tumbling lead to further contrast enhancement upon target (DNA) binding. Peptide-based agents also offer nearly unlimited synthetic flexibility in modifying and incorporating targeting motifs. We therefore tested the embedded Gd chelator design with a long-term view toward development of biological applications.

The relaxivity of GdP3W was determined at 20 and 60 MHz (37°C), and was found to be approximately 6-fold higher 60 MHz than the clinically utilized agent GdDTPA (diethylenetriamine-pentaacetic acid). Furthermore, in the presence of one equivalent of DNA, the relaxivity at 60 MHz increased by 100% to 42.4 $mM^{-1}s^{-1}$ and exhibited an unusual

field dependence. Unlike most slow tumbling complexes, the relaxivity at 60 MHz is significantly greater than at 20 MHz, and is one of the higher relaxivities reported at 60 MHz (approximately double the relaxivity of the albumin targeted contrast agent MS-325 ($23\ mM^{-1}s^{-1}$ at 60 MHz)[122]). T_1-weighted MR images (phantoms) corroborated the enhanced contrast for GdP3W over GdDTPA, and the increase in contrast upon binding DNA. Therefore these chimeras represent an entrée into new class of bifunctional targeted MRI agents with an embedded Gd site, activated by and reporting on DNA-binding.

FUTURE DIRECTIONS AND THE UTILITY OF METALLOHOMEODOMAINS

Protein design, either from first principles (*de novo*) or through redesign of known protein folds,[4] has proven to be a powerful testing ground for basic tenets of bioinorganic chemistry. We have utilized the method of "redesign" to explore native metal-binding sequences in new contexts, allowing for the interrogation of key interactions that define protein folding, DNA-interactions, and metalloenzyme reactivity.

Our approach to protein design is based on the recognition that structural elements from diverse proteins are topologically equivalent and modularly substitutable, despite very different primary sequences. We postulated that the turn of the HTH DNA-binding motif could be substituted by a metal-binding loop of another α-α corner. Our initial observation was based on the similarity of the structures of the helix-turn-helix (a DNA-binding motif), and the EF-hand (a Ca-binding motif), from which we were able to generate a chimeric metallopeptide system with unique combinations of function and selectivity. In the larger scope, the value of our research is in a) understanding the interchangability of secondary and super-secondary structure within proteins, b) developing a scaffold to manipulate DNA-binding and cleavage synergistically, and c) offering the potential to investigate the inherent reactivity of native active sites in new contexts.

With these HTH/EF-hand chimeras we have established the helix-turn-helix as a scaffold for metalloprotein design, by generating chimeric peptides incorporating metal-binding turns from physiologically unrelated sequences. The chimeras illustrate how a robust fold can be redesigned to incorporate catalytic activity into a minimalist recognition motif. We have shown that the HTH can be modified by turn-sequence

substitution to bind Ca, Ln, or other metal ions, and still retain the parental structures, and we are now exploring expanding this approach to the study of other metal-binding sites such as the Cu-prion site.[123] We have also found that the EF-hand motif can be catalytically active as single EF-hands with lanthanide ions, and have correlated activity to hydration number and Lewis acidity. Further, we have demonstrated that the HTH metallopeptides retain DNA-affinity and sequence selectivity, despite their small size. This represents the first underivatized small peptide that is a sequence-selective artificial nuclease.

The metallopeptide systems described in this review lay the groundwork for the systematic study of the basic principles of protein-DNA recognition and of enzymatic nuclease activity. Challenges remain, most notably the need to improve Ln-binding affinity or kinetic inertness, so as to retain the metals *in vivo*. Also, the ability to enhance or control reactivity will be pursued by altering inner and second-shell ligands of the metal-binding loop. As Imperiali's work showed,[52] there is great potential for metal-loop optimization through combinations of rational and combinatorial methods. Finally, the ability to deliver such systems to DNA *in situ* requires uptake or expression in cells. Because of the membrane translocation sequence of the homeodomain's HTH,[67] we have the potential for an integrated uptake signal. In preliminary studies (Louie and Franklin, unpublished data), we have found that P3W has the propensity to be taken into cells, and uptake is apparently more efficient in the presence of metals.

Among the most exciting results of these studies is the validation of our modular turn substitution approach, and the implication this has for redesign of full homeodomains. Since the HTH motif is structurally retained with the inclusion of a reactive metal-binding loop, we can construct metallo-homeodomains with the potential for even greater structural integrity and selectivity.

The next frontier in metalloprotein design is not design for its own sake, but rather utilizing this powerful tool to unravel fundamental principles governing protein structure-function relationships. By replacing or reorienting particular residue(s) at an interface, and evaluating the change in structure and reactivity of the construct, we can identify contribution of each variable in *position* and *magnitude*. Our goal is to use the metallo-homeodomain system to delineate the underlying tenets guiding DNA-sequence targeting and endonuclease activity, and to harness this understanding to create agents for gene cleavage and construction.

ACKNOWLEDGMENTS

SJF wishes to thank Profs. Kenneth N. Raymond, Jacqueline K. Barton and Sture Forsén for inspiration (fundamental, influential and coincidental, respectively) leading to this work. She also wishes to thank her co–workers, whose efforts made this research possible. This work was supported by an NSF-CAREER grant (CHE-0093000), the University of Iowa Carver Research Foundation, and the American Cancer Society (IN-122U). JTW was supported by a Center for Biocatalysis and Bioprocessing NIH Predoctoral Training Grant (T32 GM-08365). The authors thank Dr. William R. Kearney for assistance with Figure 4.

REFERENCES

1. Carrell, R. W. and B. Gooptu, 1998. Conformational changes and disease – serpins, prions and Alzheimer's. *Curr. Opin. Struct. Biol.*, **8**, 799–809.
2. Thomson, A. J. and H. B. Gray, 1998. Bio-inorganic chemistry. *Curr. Opin. Chem. Biol.*, **2**, 155–158.
3. Xing, G. and V. J. DeRose, 2001. Designing metal-peptide models for protein structure and function. *Curr. Opin. Chem. Biol.*, **5**, 196–200.
4. DeGrado, W. F., C. M. Summa, V. Pavone, F. Nastri, and A. Lombardi, 1999. De novo design and structural characterization of proteins and metalloproteins. *Annu. Rev. Biochem.*, **68**, 779–819.
5. Gibney, B. R., F. Rabanal, and P. L. Dutton, 1997. Synthesis of novel proteins. *Curr. Opin. Chem. Biol.*, **1**, 537–542.
6. Hellinga, H. W. 1998. The construction of metal centers in proteins by rational design. *Folding Des.*, **3**, R1–R8.
7. Lombardi, A., C. M. Summa, S. Geremia, L. Randaccio, V. Pavone, and W. F. DeGrado, 2000. Retrostructural analysis of metalloproteins: Application to the design of a minimal model for diiron proteins. *Proc. Nat. Acad. Sci., USA*, **97**, 6298–6305.
8. Regan, L. 1999. Protein redesign. *Curr. Opin. Struct. Biol.*, **9**, 494–499.
9. Dwyer, M. A., L. L. Looger, and H. W. Hellinga, 2004. Computational design of a biologically active enzyme. *Science*, **304**, 1967–1971.
10. Doerr, A. J. and G. L. McLendon, 2004. Design, folding, and activities of metal-assembled coiled coil proteins. *Inorg. Chem.*, **43**, 7916–7925.
11. Kaplan, J. and W. F. DeGrado, 2004. De novo design of catalytic proteins. *Proc. Nat. Acad. Sci., USA*, **101**, 11566–11570.
12. Case, M. A. and G. L. McLendon, 2004. Metal-assembled modular proteins: Toward functional protein design. *Acc. Chem. Res.*, **37**, 754–762.

13. Hellinga, H. and Richards, F. M. 1991. Construction of new ligand binding sites in proteins of known structure. I. Computer-aided modeling of sites with pre-defined geometry. *J. Mol. Biol.*, **222**, 763–785.
14. Clarke, N. D. and S. M. Yuan, 1995. Metal search: a computer program that helps design tetrahedral metal-binding sites. *Proteins: Struc. Funct. Genet.*, **23**, 256–263.
15. Desjarlais, J. R. and N. D. Clarke, 1998. Computer search algorithms in protein modification and design. *Curr. Opin. Struct. Biol.*, **8**, 471–475.
16. Benson, D. E., M. S. Wisz, and H. Hellinga, 2000. Rational design of nacent metalloenzymes. *Proc. Nat. Acad. Sci., USA*, **97**, 6292–6297.
17. Benson, D. E., A. E. Haddy, and H. W. Hellinga, 2002. Converting a maltose receptor into a nascent binuclear copper oxygenase by computational design. *Biochemistry*, **41**, 3262–3269.
18. Lu, Y., S. M. Berry, and T. D. Pfister, 2001. Engineering novel metalloproteins: design of metal-binding sites into native protein scaffolds. *Chem. Rev.*, **101**, 3047–3080.
19. Gibney, B. R., Y. Isogai, F. Rabanal, K. S. Reddy, A. M. Grosset, C. C. Moser, and P. L. Dutton, 2000. Self-assembly of heme A and heme B in a designed four-helix bundle: Implications for a cytochrome c oxidase maquette. *Biochemistry*, **39**, 11041–11049.
20. Gibney, B. R., S. E. Mulholland, F. Rabanal, and P. L. Dutton, 1996. Ferredoxin and ferredoxin-heme maquettes. *Proc. Natl. Acad. Sci., USA*, **93**, 15041–15046.
21. Kennedy, M. L. and B. R. Gibney, 2001. Metalloprotein and redox protein design. *Curr. Opin. Struct. Biol.*, **11**, 485–490.
22. Zhuang, J., J. H. Amoroso, R. Kinloch, J. H. Dawson, M. J. Baldwin, and B. R. Gibney, 2004. Design of a five-coordinate heme protein maquette: A spectroscopic model of deoxy myoglobin. *Inorg. Chem.*, **43**, 8218–8220.
23. Turano, P. and Y. Lu, 2001. Iron in Heme and Related Proteins. In *Handbook on Metalloproteins*, eds. I. Bertini, H. Sigel, and A. Sigel, New York, Marcel Dekker, pp 269–356.
24. Gehring, W. J., M. Affolter, and T. Bürglin, 1994. Homeodomain proteins. *Annu. Rev. Biochem.*, **63**, 487–526.
25. Laughon, A. 1991. DNA binding specificity of homeodomains. *Biochemistry*, **30**, 11357–11367.
26. Lu, Y., L. B. LaCroix, M. D. Lowery, E. I. Solomon, C. J. Bender, J. Peisach, J. A. Roe, E. B. Gralla, and J. S. Valentine, 1993. Construction of a 'blue' copper site at the native zinc site of yeast copper-zinc superoxide dismutase. *J. Am. Chem. Soc.*, **115**, 5907–5918.
27. Lu, Y., J. A. Roe, C. J. Bender, J. Peisach, L. Banci, I. Bertini, E. B. Gralla, and J. S. Valentine, 1996. New Type 2 copper-cysteinate proteins. Copper

site his-to-cysteine mutants of yeast copper-zinc superoxide dismutase. *Inorg. Chem*., **35**, 1692–1700.
28. Winkler, J. R., P. Wittung-Stafshede, J. Leckner, B. G. Malmstrom, and H. B. Gray, 1997. Effects of folding on metalloprotein active sites. *Proc. Nat. Acad. Sci., USA*, **94**, 4246–4249.
29. Sigman, J. A., H. K. Kim, X. Zhao, J. R. Carey, and Y. Lu, 2003. The role of copper center and protons in heme-copper oxidases: Kinetic study of an engineered heme-copper center in myoglobin. *Proc. Nat. Acad. Sci., USA*, **100**, 3629–3634.
30. Nomura, A. and Y. Sugiura, 2004. Hydrolytic reaction by zinc finger mutant peptides: Successful redesign of structural zinc sites into catalytic zinc sites. *Inorg. Chem*., **43**, 1708–1713.
31. Nomura, A. and Y. Sugiura, 2004. Sequence-selective and hydrolytic cleavage of DNA by zinc finger mutants. *J. Am. Chem. Soc*., **126**, 15374–15375.
32. Efimov, A. V. 1996. A structural tree for a-helical proteins containing α-α-corners and its application to protein classification. *FEBS Lett*., **391**, 167–170.
33. Falke, J. J., E. E. Snyder, K. C. Thatcher, and C. S. Voertler, 1991. Quantitating and engineering the ion specificity of an EF-hand-like Ca^{2+} binding site. *Biochemistry*, **30**, 8690–8697.
34. Dudev, T. and C. Lim, 2003. Principles governing Mg, Ca, and Zn binding and selectivity in proteins. *Chem. Rev*., **103**, 773–787.
35. Kretsinger, R. H. and C. E. Nockolds, 1973. Carp muscle calcium-binding protein. II. Structure determination and general description. *J. Biol. Chem*., **248**, 3313–3326.
36. Berridge, M. J., M. D. Bootman, and H. L. Roderick, 2003. Calcium signalling: Dynamics, homeostasis and remodelling. *Nature Rev. Mol. Cell Biol*., **4**, 517–529.
37. Falke, J. J., S. K. Drake, A. L. Hazard, and O. B. Peersen, 1994. Molecular tuning of ion binding to calcium signaling proteins. *Quart. Rev. Biophys*., **27**, 219–290.
38. Drake, S. K. and J. J. Falke, 1996. Kinetic tuning of the EF-hand calcium binding motif: The gateway residue independently adjusts (i) barrier height and (ii) equilibrium. *Biochemistry*, **35**, 1753–1760.
39. Drake, S. K., K. L. Lee, and J. J. Falke, 1996. Tuning the equilibrium ion affinity and selectivity of the EF-hand calcium binding motif: Substitutions at the gateway position. *Biochemistry*, **35**, 6697–6705.
40. Horrocks, W. D., Jr. 1993. Luminescence spectroscopy. *Meth. Enzym*., **226**, 495–538.
41. Pidcock, E. and G. R. Moore, 2001. Structural characteristics of protein binding sites for calcium and lanthanide ions. *J. Biol. Inorg. Chem*., **6**, 479–489.

42. Burroughs, S. E., W. D. Horrocks, Jr., H. Ren, and C. Klee, 1994. Characterization of the lanthanide ion-binding propertides of Calcineurin-B using laser-induced luminescence spectroscopy. *Biochemistry*, **33**, 10428–10436.
43. Yang, W., H.-W. Lee, H. Hellinga, and J. T. Yang, 2002. Structural analysis, identification, and design of calcium-binding sites in proteins. *Proteins: Struc. Funct. Genet.*, **47**, 344–356.
44. Kawasaki, H., S. Nakayama, and R. H. Kretsinger, 1998. Classification and evolution of EF-hand proteins. *Biometals*, **11**, 277–295.
45. Yang, W., L. M. Jones, L. Isley, Y. Ye, H. W. Lee, A. Wilkins, Z. Liu, H. W. Hellinga, R. Malchow, M. Ghazi, and J. J. Yang, 2003. Rational design of a calcium binding protein. *Journal of the American Chemical Society*, **125**, 6165–6171.
46. Vázquez-Ibar, J. L., A. B. Weinglass, and H. R. Kaback, 2002. Engineering a terbium-binding site into an integral membrane protein for luminescence energy transfer. *Proc. Nat. Acad. Sci., USA*, **99**, 3487–3492.
47. Procyshyn, R. M. and R. E. Reid, 1994. A structure/activity study of calcium affinity and selectivity using a synthetic peptide model of the helix-loop-helix calcium-binding motif. *J. Biol. Chem.*, **269**, 1641–1647.
48. Gariépy, J., B. D. Sykes, and R. S. Hodges, 1983. Lanthanide-induced peptide folding: Variations in lanthanide affinity and induced peptide conformation. *Biochemistry*, **22**, 1765–1772.
49. Wójcik, J., J. Góral, K. Pawlowski, and A. Bierzynski, 1997. Isolated calcium-binding loops of EF-hand proteins can dimerize to form a native-like structure. *Biochemistry*, **36**, 680–687.
50. Glusker, J. P. 1991. Structural aspects of metal liganding to functional-groups in proteins. *Advances in Protein Chemistry*, **42**, 1–76.
51. Bonagura, C. A., M. Sundaramoorthy, and T. L. Poulos, 1999. Conversion of an engineered potassium-binding site into a calcium-selective site in cytochrome *c* peroxidase. *J. Biol. Chem.*, **274**, 37827–37833.
52. Nitz, M., K. J. Franz, R. L. Maglathlin, and B. Imperiali, 2003. A powerful combinatorial screen to identify high-affinity Terbium(III)-binding peptides. *ChemBioChem.*, **4**, 272–276.
53. Franz, K. J., M. Nitz, and B. Imperiali, 2003. Lanthanide-binding tags as versatile protein coexpression probes. *ChemBioChem.*, **4**, 265–271.
54. Rebar, E. J., Y. Huang, R. Hickey, A. K. Nath, D. Meoli, S. Nath, B. Chen, L. Xu, Y. Liang, A. C. Jamieson, L. Zhang, S. K. Spratt, C. C. Case, A. Wolffe, and F. J. Giordano, 2002. Induction of angiogenesis in a mouse model using engineered transcription factors. *Nat. Med.*, **8**, 1427–1432.
55. Pabo, C. O., J. Peisach, and R. A. Grant, 2001. Design and selection of novel Cys_2His_2 zinc finger proteins. *Annu. Rev. Biochem.*, **70**, 313–340.
56. Montclare, J. K. and A. Schepartz, 2003. Miniature homeodomains: High specificity without an N-terminal arm. *J. Am. Chem. Soc.*, **125**, 3416–3417.

57. Hori, Y. and Y. Sugiura, 2002. Conversion of antennapedia homeodomain to zinc finger-like domain: Zn(II)-induced change in protein conformation and DNA Binding. *J. Am. Chem. Soc.*, **124**, 9362–9363.
58. Derossi, D., A. H. Joliot, G. Chassaing, and A. Prochiantz, 1994. The third helix of the antennapedia homeodomain translocates through biological membranes. *J. Biol. Chem.*, **269**, 10444–10450.
59. Ledneva, R. K., A. V. Alexeevskii, S. A. Vasil'ev, S. A. Spirin, and A. S. Karyagina, 2001. Structural aspects of interaction of homeodomains with DNA. *Molecular Biol.*, **35**, 647–659.
60. Treisman, J., E. Harris, D. Wilson, and C. Desplan, 1992. The homeodomain: A new face for the helix-turn-helix. *BioEssays*, **14**, 145–150.
61. Kissinger, C. R., B. Lui, E. Martin-Blanco, T. B. Kornberg, and C. O. Pabo, 1990. Crystal structure of an engrailed homeodomain-DNA complex at 2.8 angstroms resolution: A framework for understanding homeodomain-DNA interactions. *Cell*, **63**, 579–590.
62. Burley, S. K. 1994. DNA-binding motifs from eukaryotic transcription factors. *Curr. Opin. in Struct. Biol.*, **4**, 3–11.
63. Wintjens, R. and M. Rooman, 1996. Structural classification of HTH DNA-binding domains and protein-DNA interaction modes. *J. Mol. Biol.*, **262**, 294–313.
64. Clarke, N. D. 1995. Covariation of residues in the homeodomain sequence family. *Protein Sci.*, **4**, 2269–2278.
65. Banerjee-Basu, S., T. Moreland, B. J. Hsu, K. L. Trout, and A. D. Baxevanis, 2003. The homeodomain resource: 2003 update. *Nucleic Acids Res.*, **31**, 304–306.
66. Dom, G., C. Shaw-Jackson, C. Matis, O. Bouffioux, J. J. Picard, A. Prochiantz, M.-P. Mingeot-Leclercq, R. Brasseur, and R. Rezsohazy, 2003. Cellular uptake of Antennapedia Penetratin peptides is a two-step process in which phase transfer precedes a tryptophan-dependent translocation. *Nucleic Acids Res.*, **31**, 556–561.
67. Prochiantz, A. 2000. Messenger proteins: homeoproteins, TAT and others. *Curr. Opin. Cell Biol.*, **12**, 400–406.
68. Sreedhara, A. and J. A. Cowan, 2001. Catalytic hydrolysis of DNA by metal ions and complexes. *J. Biol. Inorg. Chem.*, **6**, 337–347.
69. Schneider, H.-J. and A. K. Yatsimirsky, 2003. Lanthanide-catalyzed hydrolysis of phosphate esters and nucleic acids. In *Metals in Biological Systems*, eds., H. Sigel and A. Sigel, New York, Marcel Dekker, Inc., Vol. 40, pp. 369–462.
70. Franklin, S. J. 2001. Lanthanide mediated DNA hydrolysis. *Curr. Opin. Chem. Biol.*, **5**, 201–208.

71. Komiyama, M. 1999. Hydrolysis of DNA and RNA by lanthanide ions: mechanistic studies leading to new applications. *Chem. Commun*., **16**, 1443–1451.
72. Chappell, L. L., D. A. Voss, W. D. Horrocks, Jr., and J. R. Morrow, 1998. Effect of mixed pendent groups on the solution and catalytic properties of Europium(III) macrocyclic complexes: Bifunctional and monfunctional amide and alcohol pendents in septadentate or octadentate ligands. *Inorg. Chem*., **37**, 3989–3998.
73. Koa, C. and J. R. Morrow, 1997. RNA cleavage and phosphate diester transesterification by encapsulated lanthanide ions: Traversing the lanthanide series with Lanthanum(III), Europium(III), and Lutetium(III) complexes of 1,4,7,10-Tetrakis(2-Hydroxyalkyl)-1,4,7,10-Tetraazacyclododecane. *Inorg. Chem*., **33**, 5036–5041.
74. Baker, B. M., H. Khalili, N. Wei, and J. R. Morrow, 1997. Cleavage of the 5' cap structure of mRNA by a europium(III) macrocyclic complex with pendant alcohol groups. *J. Am. Chem. Soc.*, **119**, 8749–8755.
75. Huang, L., L. L. Chappel, O. Irazo, B. F. Baker, and J. R. Morrow, 2000. Oligonucleotide conjugates of Eu(III) tetraazamacrocycles with pendent alcohol and amide groups promote sequence-specific RNA cleavage. *JBIC* **5**, 85–92.
76. Komiyama, M. 1995. Sequence-specific and hydrolytic scission of DNA and RNA by lanthanide complex-oligoDNA hybrids. *J. Biochem*., **118**, 665–670.
77. Chen, W., Y. Kitamura, J. M. Zhou, J. Sumaoka, and M. Komiyama, 2004. Site-selective DNA hydrolysis by combining Ce(IV)/EDTA with monophosphate-bearing oligonucleotides and enzymatic ligation of the scission fragments. *J. Am. Chem. Soc.*, **126**, 10284–10291.
78. Welch, J. T., W. R. Kearney, and S. J. Franklin, 2003. Lanthanide-binding HTH peptides: solution structure of a designed metallonuclease. *Proc. Nat. Acad. Sci., USA*, **100**, 3725–3730.
79. Chattopadhyaya, R., W. E. Meador, A. R. Means, and F. A. Quiocho, 1992. Calmodulin structure refined at 1.7 Angstroms resolution. *J. Mol. Biol*., **228**, 1177–1192.
80. Guex, N. and M. C. Peitsch, 1997. SWISS-MODEL and the Swiss-PdbViewer: An environment for comparative protein modeling. *Electrophoresis*, **18**, 2714–2723.
81. Lindahl, E., B. Hess, and D. van der Spoel, 2001. GROMACS 3.0: A package for molecular simulation and trajectory analysis. *J. Mol. Mod*., **7**, 306–317.
82. Kim, Y., J. T. Welch, K. M. Lindstrom, and S. J. Franklin, 2001. Chimeric HTH motifs based on EF-hands. *J. Biol. Inorg. Chem*., **6**, 173–181.

83. Sirish, M. and S. J. Franklin, 2002. Hydrolytically active Eu(III) and Ce(IV) EF-hand peptides. *J. Inorg. Biochem*., **91**, 253–258.
84. Sirish, M. and H.-J. Schneider, 1999. Supramolecular chemistry, part 86-Porphyrin derivatives as water-soluble receptors for peptides. *Chem. Commun*., 907–908.
85. Stollar, E. J., U. Mayor, S. C. Lovell, L. Federici, S. M. V. Freund, A. R. Fersht, and B. F. Luisi, 2003. Crystal structures of engrailed homeodomain mutants. *J. Biol. Chem*., **278**, 43699–43708.
86. Stollar, E. J., J. L. Gelpi, S. Velankar, A. Golovin, M. Orozco, and B. F. Luisi, 2004. Unconventional interactions between water and heterocyclic nitrogens in protein structures. *Proteins: Struc. Funct. Genet*., **57**, 1–8.
87. Adams, P. D., Y. Chen, K. Ma, M. G. Zagorski, F. D. Sonnichsen, M. L. McLaughlin, and M. D. Barkley, 2002. Intramolecular quenching of tryptophan fluorescence by the peptide bond in cyclic hexapeptides. *J. Am. Chem. Soc*., **124**, 9278–9286.
88. Pfefferle, J.-M. and J.-C. G. Bünzli, 1989. Interaction between the Buffer Tris and the Eu(III) Ion: Luminescence and potentiometric investigation. *Helv. Chem. Acta*., **72**, 1487–1494.
89. Dadlez, M., J. Góral, and A. Bierzynski, 1991. Luminescence of peptide-bound terbium ions. Determination of binding constants. *FEBS Lett*., **282**, 143–146.
90. Marsden, B. J., G. S. Shaw, and B. D. Sykes, 1990. Calcium binding proteins: Elucidating the contributions to calcium affinity from an analysis of species varients and peptide fragments. *Biochem. Cell Biol*., **68**, 587–601.
91. Welch, J. T. 2004. The structural characterization of EF-hand chimeras based on the helix-turn-helix. Ph.D. Dissertation, University of Iowa, Iowa City, IA.
92. Drake, S. K., M. A. Zimmer, C. Kundrot, and J. J. Falke, 1997. Molecular tuning of an EF-hand-like calcium binding loop: Contributions of the coordinating side chain at Loop Position 3. *J. Gen. Physiol*., **110**, 173–184.
93. Lehrman, S. R., J. L. Tuls, and M. Lund, 1990. Peptide alpha-helicity in aqueous trifluoroethanol—correlations with predicted alpha-helicity and the secondary structure of the corresponding regions of bovine growth-hormone. *Biochemistry*, **29**, 5590–5596.
94. Mayor, U., J. G. Grossman, N. W. Foster, S. M. V. Freund, and A. R. Fersht, 2003. The denatured state of engrailed homeodomain under denaturing and native conditions. *J. Mol. Biol*., **333**, 977–991.
95. Luo, P. and R. L. Baldwin, 1997. Mechanism of helix induction by Trifluoroethanol: A framework for extrapolating the helix-forming properties of peptides from Trifluoroethanol/water mixtures back to water. *Biochemistry*, **36**, 8413–8421.

96. Shaw, G. S., R. S. Hodges, and B. D. Sykes, 1990. Calcium-induced peptide association to form an intact protein domain: 1H NMR structural evidence. *Science*, **249**, 280–283.
97. Shaw, G. S. and B. D. Sykes, 1996. NMR solution structure of a synthetic Troponin C heterodimeric domain. *Biochemistry*, **35**, 7429–7438.
98. Akke, M., S. Forsén, and W. J. Chazin, 1991. Molecular basis for cooperativity in Ca^{2+} binding to calbindin D_{9k}. *J. Mol. Biol.*, **220**, 173–189.
99. Wishart, D. S., B. D. Sykes, and F. M. Richards, 1992. The chemical shift index: A fast and simple method for the assignment of protein secondary structure through NMR spectroscopy. *Biochemistry*, **31**, 1647–1651.
100. Merutka, G., H. J. Dyson, and P. E. Wright, 1995. 'Random coil' ^1H chemical shifts obtained as a function of temperature and trifluoroethanol concentration for the peptide series GGXGG. *J. Biomol. NMR*, **5**, 14–24.
101. Jain, S., J. T. Welch, W. D. Horrocks, Jr., and S. J. Franklin, 2003. Europium luminescence of EF-hand HTH chimeras: Impact of pH and DNA-binding on europium coordination. *Inorg. Chem.*, **42**, 8098–8104.
102. Horrocks, W. D., Jr. and D. R. Sudnick, 1981. Lanthanide ion luminescence probes of the structure of biological macromolecules. *Acc. Chem. Res.*, **14**, 384–392.
103. McNemar, C. W. and W. D, Horrocks, Jr. 1989. The resolution of laser-induced Europium(III) ion excitation-spectra through the use of the Marquardt Nonlinear-Regression Method. *Appl. Spectrosc.*, **43**, 816–821.
104. Supkowski, R. M. and W. D. Horrocks, Jr. 2002. On the determination of the number of water molecules, *q*, coordinated to europium(III) ions in solution from luminescence decay lifetimes. *Inorg. Chim. Acta.*, **340**, 44–48.
105. Wu, S. L., S. J. Franklin, K. N. Raymond, and W. D. Horrocks, Jr. 1996. Kinetics of the formation of macrocyclic polyaminocarboxylate ligand complexes: A laser-excited luminescence study of the Eu^{3+}-dtpa-dien system. *Inorg. Chem.*, **35**, 162–167.
106. Dunand, F. A. and A. E. Merbach, 2001. UV-Vis observation of different $^7F_0$ $^5D_0$ transitions for both isomeric species in Eu(III) DOTA-like complexes. *Inorg. Chem. Commun.*, **4**, 719–722.
107. Henzl, M. T. and E. R. Birnbaum, 1988. Oncomodulin and Parvalbumin. *J. Biol. Chem.*, **263**, 10674–10680.
108. Kauffman, J. F., R. C. Hapak, and M. T. Henzl, 1995. Interconversion of the CD and EF sites in oncomodulin. Influence on the Eu^{3+} $^7F_0{}^5D_0$ excitation spectrum. *Biochemistry*, **34**, 991–1000.
109. Henzl, M. T., C. L. Treviño, L. Dvoråkovå, and J. M. Boschi, 1992. Evidence that deprotonation of Serine-55 is responsible for the pH-dependence of the parvalbumin Eu^{3+} $^7F_0$ $^5D_0$ Spectrum. *FEBS Lett.*, **314**, 130–134.

110. Christianson, D. W. and C. A. Fierke, 1996. Carbonic anhydrase: Evolution of the zinc binding site by nature and by design. *Acc. Chem. Res.*, **29**, 331–339.
111. Welch, J. T., M. Sirish, K. M. Lindstrom, and S. J. Franklin, 2001. *De Novo* nucleases based on HTH and EF-hand chimeras. *Inorg. Chem.*, **40**, 1982–1984.
112. Kovacic, R. T., J. T. Welch, and S. J. Franklin, 2003. Sequence preference in DNA cleavage by a chimeric metallopeptide. *J. Am. Chem. Soc.*, **125**, 6656–6662.
113. Komiyama, M., N. Takeda, Y. Takahashi, H. Uchida, T. Shiiba, T. Kodama, and M. Yashiro, 1995. Efficient and oxygen-independent hydrolysis of single-stranded DNA by Cerium(IV) Ion. *J. Chem. Soc., Perkin Trans.*, **2**, 269–274.
114. Branum, M. E., A. K. Tipton, S. Zhu, and L. Que, Jr. 2001. Double-strand hydrolysis of plasmid DNA by dicerium complexes at 37°C. *J. Am. Chem. Soc.*, **123**, 1898–1904.
115. Branum, M. E. and L. Que, Jr., 1999. Double-strand DNA hydrolysis by dilanthanide complexes. *J. Biol. Inorg. Chem.*, **4**, 593–600.
116. Zondlo, N. J. and A. Schepartz, 1999. Highly specific DNA recognition by a designed miniature protein. *J. Am. Chem. Soc.*, **121**, 6938–6939.
117. McColl, D. J., C. D. Honchell, and A. D. Frankel, 1999. Structure-based design of an RNA-binding zinc finger. *Proc. Nat. Acad. Sci., USA*, **96**, 9521–9526.
118. Copeland, K. D., M. P. Fitzsimons, R. P. Houser, and J. K. Barton, 2002. DNA hydrolysis and oxidative cleavage by metal-binding peptides tethered to rhodium intercalators. *Biochemistry*, **41**, 343–356.
119. Hori, Y., K. Suzuki, Y. Okuno, M. Nagaoka, S. Futaki, and Y. Sugiura, 2000. Artificial zinc finger peptide containing a novel His4 domain. *J. Am. Chem. Soc.*, **122**, 7648–7653.
120. Louie, A. Y., M. M. Hüber, E. T. Ahrens, U. Rothbächer, R. Moats, R. E. Jacobs, S. E. Fraser, and T. J. Meade, 2000. In vivo visualization of gene expression using magnetic resonance imaging. *Nature Biotech.*, **18**, 321–325.
121. Caravan, P., J. M. Greenwood, J. T. Welch, and S. J. Franklin, 2003. Gadolinium-binding helix-turn-helix peptides: DNA-dependent MRI contrast agents. *Chem. Commun.*, 2574–2575.
122. Caravan, P., N. J. Cloutier, M. T. Greenfield, S. A. McDermid, S. U. Dunham, J. W. M. Bulte, J. C. Amedio, Jr., R. J. Looby, R. M. Supkowski, W. D. Horrocks, Jr., T. J. McMurry, and R. B. Lauffer, 2002. The interaction of MS-325 with human serum albumin and its effect on proton relaxation rates. *J. Am. Chem. Soc.*, **124**, 3152–3162.
123. Shields, S. B. and S. J. Franklin, 2004. De novo design of a Cu(II)-binding helix-turn-helix chimera: The prion octarepeat motif in a new context. *Biochemistry*, **43**, 16086–16091.